SIMULATION STUDIES OF PARAMETRIC AMPLIFICATION IN BIO-INSPIRED FLOW SENSORS

H. Droogendijk[1] and G. J. M. Krijnen[1]

[1] *University of Twente, MESA+ Research Institute; P.O. Box 217, 7500 AE, Enschede, The Netherlands*

***Abstract* — In this paper the effect of parametric amplification in MEMS-based air-flow hair-sensors is studied. With an AC-voltage controlled torsional stiffness the rotation of the hair can be influenced. With the appropriate amplitude, phase and frequency, the rotation of the torsional hair system is increased with respect to the case without parametric amplification. Therefore, parametric amplification is identified as a method to improve the performance of MEMS-based hair air flow sensors.**

***Keywords:* Cricket hair, Bio-inspired, Flow sensor, Non-linear effects, Parametric amplification**

I – Introduction

Inspired by crickets (figure 1) and their exquisite perception of flow phenomena down to thermal noise levels [1], artificial hair-based flow sensors have been developed successfully in our group [2]. The realization of array structures and improvement of fabrication methodologies have led to better performance, making it possible to measure (illustrated in figure 2) sub-mm/s flow velocities [3]. To further improve the performance of these artificial hair flow sensors, we propose to make use of non-linear effects. In nature a wide range of such effects exist (filtering, parametric amplification, etc.) giving improvements in sensitivity, dynamic range and selectivity.

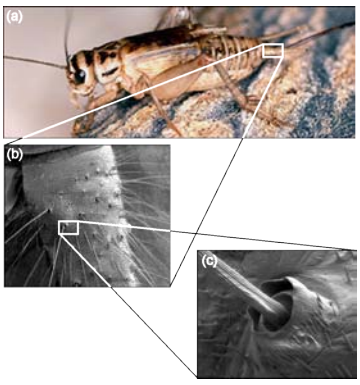

Figure 1: *Flow perception by crickets (SEM pictures courtesy of Jérôme Casas, Université de Tours).*

II – Parametric amplification

Parametric amplification (PA) is based on a nonlinear response of a material or structure to excitation. Due to this nonlinearity the simultaneous presence of more than one excitation signal will in general lead to a complex interaction where amplitude, frequency and phase of each of the excitatory signals play important roles in the entanglement of the signals and the overall response. In the case of our capacitive hair-based flow sensors, which are in fact electrostatic transducers, we have the freedom to apply electrostatic torques in addition to the flow driven torques. The former causes the flow-sensing capabilities of the sensor to be modulated and this can be considered as adaptation of the sensor performance. By controlling the mechanical properties of the hair sensory system in time an interesting dynamical system can be obtained. It is shown that with the appropriate choice of parameters the input is amplified by the system compared to the case without parametric amplification [4]. Generally, with a well-defined configuration one can achieve filtering and selective gain of the system.

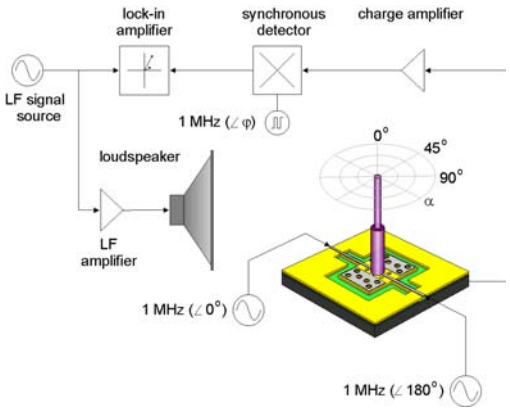

Figure 2: *Performing flow measurements with artificial hair-sensors.*

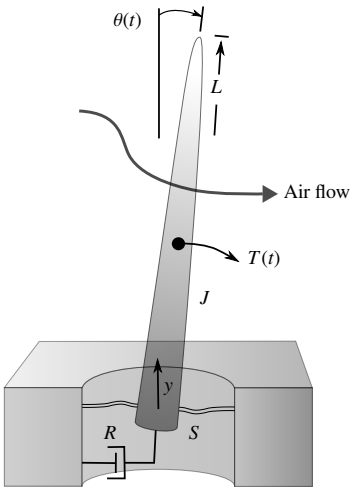

Figure 3: *Model of a flow sensing hair [5].*

To investigate how this principle can be used in our bio-inspired hair sensor (figure 3), we consider the second-order differential equation describing its behavior, where J is the moment of inertia, R the torsional resistance, S the torsional stiffness, T the drag torque amplitude due to oscillating air flow with angular frequency ω_a (=$2\pi f_a$):

$$J\frac{d^2\theta}{dt^2} + R\frac{d\theta}{dt} + S(t)\theta = T_0\cos(\omega_a t) \qquad (1)$$

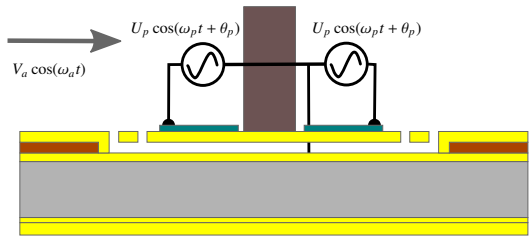

Figure 4: *Modulating the torsional spring stiffness in time.*

Note that J and R may contain contributions due to air flow viscous and inertial effects. Normally the torsional stiffness is given by a spring constant. But it may well be modulated in time applying an AC voltage on the two capacitor plates of the sensors. Assume this signal has amplitude U_p, frequency ω_p (=$2\pi f_p$) and phase ϕ_p (illustrated in figure 4):

$$S(t) = S_0 - \frac{1}{4}U_p^2\frac{d^2C}{d\theta^2} - \frac{1}{4}U_p^2\cos(2\omega_p t + 2\phi_p)\frac{d^2C}{d\theta^2} \qquad (2)$$

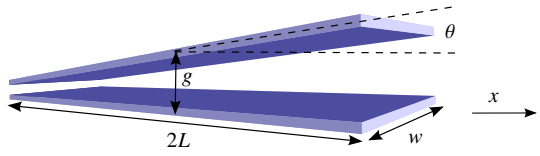

Figure 5: *Tilted rectangular capacitor.*

The capacitance C is calculated from the sensor geometry, which is considered as a tilted rectangular plate (figure 5). For this configuration, $2L$ is the length of the membrane, w is the width of the membrane, g is the distance between the (rotational) center of the membrane and the substrate and θ is the rotation angle. The capacitance $C(\theta)$ as function of the rotation angle is:

$$C(\theta) = \int_{-L}^{L}\frac{\epsilon_0 w\cos(\theta)}{g - x\sin(\theta)}dx \qquad (3)$$

Approximation of its solution by a second order Taylor expansion leads to:

$$C(\theta) \approx \frac{\epsilon_0 w 2L}{g}\left(1 + \frac{1}{6}\left(\frac{2L^2}{g^2} - 1\right)\theta^2\right) + O(\theta^4) \qquad (4)$$

where the first and third order in θ drop because of symmetry of the capacitor geometry. Using this approximation, the value for $\frac{d^2C}{d\theta^2}$ in equation 2 can be calculated for small values of the rotation angle θ.

An analytical solution for equation 1 with $S(t)$ given by equation 2 is hard to obtain. According to [6] the solution of this differential equation contains an infinite series of odd harmonics with respect to the pump frequency ω_p. Therefore, we use the Runge-Kutta 4 method from MATLAB to solve the differential equation numerically. In order to use this numerical method, the differential equation is converted to a set of linear first-order differential equations in state space:

$$\begin{bmatrix}\dot{\boldsymbol{\alpha}}_1(t)\\ \dot{\boldsymbol{\alpha}}_2(t)\end{bmatrix} = \begin{bmatrix}0 & 1\\ -\frac{S(t)}{J} & -\frac{R}{J}\end{bmatrix}\begin{bmatrix}\boldsymbol{\alpha}_1(t)\\ \boldsymbol{\alpha}_2(t)\end{bmatrix} + \begin{bmatrix}0\\ \frac{T_0}{J}\end{bmatrix}\boldsymbol{u}(t) \qquad (5)$$

where

$$\boldsymbol{\theta}(t) = \begin{bmatrix}1 & 0\end{bmatrix}\begin{bmatrix}\boldsymbol{\alpha}_1(t)\\ \boldsymbol{\alpha}_2(t)\end{bmatrix} \qquad \boldsymbol{u}(t) = \cos(\omega_a t) \qquad (6)$$

In these equations, $\boldsymbol{\alpha}_1(t)$ represents the rotation angle of the hair, $\boldsymbol{\alpha}_2(t) = \dot{\boldsymbol{\alpha}}_1(t)$ is the angular velocity of the hair, $\dot{\boldsymbol{\alpha}}_2(t) = \ddot{\boldsymbol{\alpha}}_1(t)$ is the acceleration of the hair and the output $\boldsymbol{\theta}(t)$ is the rotation angle of the hair.

To determine the occurrence of parametric amplification experimentally the pump parameters need to be chosen judiciously. The hair sensor is suspended by two silicon nitride beams ideally allowing for torsional movement only. However, in practice the beams also have a vertical compliance due to finite stiffness in that direction, which is illustrated in figure 6.

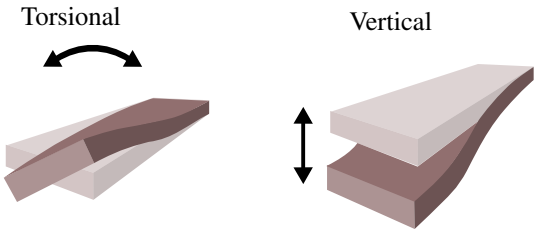

Figure 6: *Two types of stiffness.*

Since parametric amplification is implemented by applying voltages, leading to vertical forces and torques, the entire membrane structure also moves in the vertical direction. Using the Fourier transform method to determine the effect of parametric amplification on the gain at the flow frequency component ω_a in the resulting spectrum, contributions from vertical movement (as a consequence from finite vertical stiffness) are undesired and should be minimized, especially at that frequency component.

III – Simulation results

To perform the simulations in MATLAB, the data for the MEMS-based hair flow sensor from tabel 1 is used.

Table 1: *Properties of a MEMS hair sensor.*

Quantity	Symbol	Value	Unit
Torsional stiffness	S	$5.2 \cdot 10^{-9}$	N · m/rad
Torsional resistance	R	$1.68 \cdot 10^{-12}$	N · m/rad/s
Moment of inertia	J	$1.97 \cdot 10^{-16}$	kg · m^2
Capacitor gap	g	600	nm
Capacitor width	w	90	µm
Capacitor length	L	95	µm

The initial values for the input air flow parameters and the AC voltage (which is denoted ”pump”) parameters, are listed in table 2. The drag torque calculations for T_0 are based on 40 mm/s flow using Stokes' mechanical impedance for oscillating air flow [5].

Table 2: *Simulation parameters.*

Quantity	Symbol	Value	Unit
Drag torque amplitude	T_0	$4.69 \cdot 10^{-13}$	N · m
Flow frequency	f_a	80	Hz
Pump amplitude	U_p	1	V
Pump angle	ϕ_p	0	degree
Pump frequency	f_p	80	Hz

The pump frequency f_p is chosen in such a way that the output signal does not contain a component of vertical movement at the air flow frequency f_a, using the relationship for the electrically generated force F_p in the vertical direction y:

$$F_p = \frac{1}{2}U^2\frac{dC}{dy} = \frac{U_p^2}{4}\frac{dC}{dy}\left(1 + \cos(2\omega_p t + 2\phi_p)\right) \quad (7)$$

To state the effect of parametric amplification on the sensory system performance, the gain G is defined as the ratio of the amplitudes of the angular rotation with and without pump:

$$G = \frac{\theta_{0,\text{with pump}}}{\theta_{0,\text{without pump}}} \quad (8)$$

With the simulation parameters given, first the effect of the pump phase ϕ_p with respect to the air flow frequency on the gain G is determined. The resulting plot is given in figure 7.

The effect of changing the pump phase ϕ_p can be seen clearly, resulting in a gain varying from about 1.12 to 1.44. The sinusoidal shape can be explained as a spring that becomes weaker when the torque is large compared to the case that the spring is weak when the torque is small. Note that the case without parametric amplification has a gain of 1 ($U_p = 0$).

Also, the pump amplitude U_p affects the strength of parametric amplification, which is also the case when applying electrostatic spring softening by a DC voltage.

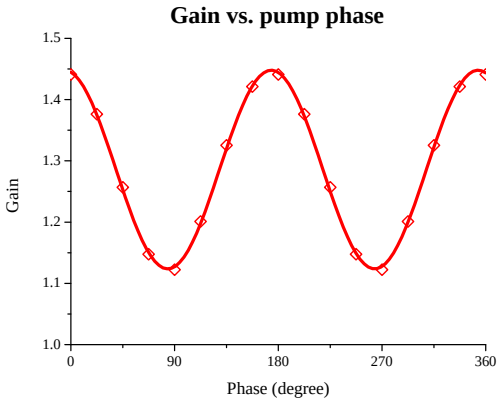

Figure 7: *Gain vs. pump phase ϕ_p.*

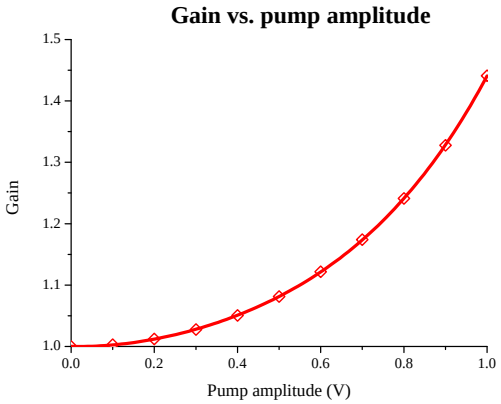

Figure 8: *Gain vs. pump amplitude U_p.*

The relationship between the pump amplitude U_p and the resulting gain G is given in figure 8 for $\phi_p = 0$.

In this plot a non-linear relation between the pump amplitude U_p and gain G is observed, where a gain of about 1.44 is obtained at a pump amplitude of 1 V. The pump amplitude cannot be increased too much, because pull-in occurs when the voltage between the capacitor plates becomes too high.

Parametric amplification can lead to selective gain and thus additional filtering of the system, which is determined by investigating the relationship between the pump frequency f_p and the resulting gain G (figure 9).

From this plot we observe that at pumping at half the air flow frequency f_a the gain is increased a little (from 1.29 to 1.31) with respect to pump frequencies f_p in the same region, but especially when pumping with the same frequency f_p as the air flow frequency f_a (from 1.29 to 1.44, which is about 12%). From equation 2 this means that varying the torsional stiffness $S(t)$ with twice the frequency of the incoming air flow (f_p=f_a) leads to significant gain G. Other frequencies

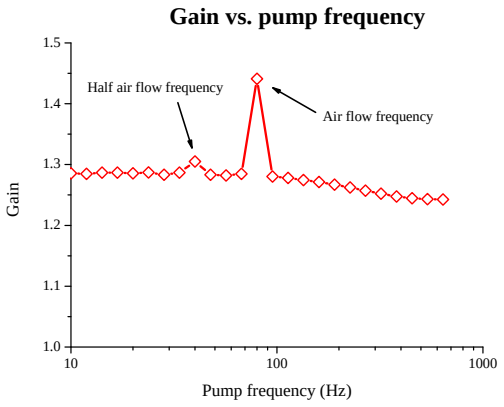

Figure 9: *Gain vs. pump frequency f_p.*

also show a gain larger than 1, as a consequence of non-synchronized spring softening and the presence of the DC-component in the voltage squared term (see equation 2).

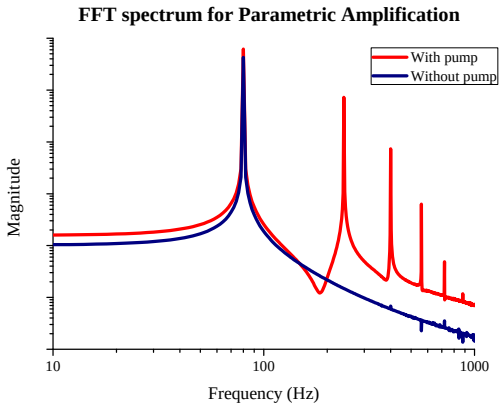

Figure 10: *FFT spectrum of the rotation angle with (red curve) and without (blue curve) presence of a pump signal.*

By inspection of the angular rotation spectrum in the presence of the pump signal, we observe the occurrence of odd harmonics in the solution (figure 10). Therefore, when performing measurements the gain due to parametric amplification should be determined based on the strength of the flow frequency component by means of a Fourier Transform rather than using the RMS-value for the entire spectrum (also containing undesired vertical movement).

IV – Conclusions

By exploiting the non-linearity of our artificial hair sensory system for measuring oscillating air flow, the performance of these sensors can be further improved. Parametric amplification is identified to be a useful mechanism for improving the flow perception and for allowing filtering by selective gain of the sensor system, using appropriate pump amplitude, phase and frequency.

References

[1] Tateo Shimozawa, Jun Murakami, and Tseneko Kumagai. *Sensors and Sensing in Biology and Engineering*, chapter 10. Cricket Wind Receptors: Thermal Noise for the Highest Sensitivity Known, pages 145–156. Springer, Wien, Austria, 2003.

[2] M. A. Dijkstra, J. J. J. van Baar, R. J. Wiegerink, T. S. J. Lammerink, J. H. de Boer, and G. J. M. Krijnen. Artificial sensory hairs based on the flow sensitive receptor hairs of crickets. *Journal of micromechanics and microengineering*, 15:S132–S138, July 2005.

[3] C. M. Bruinink, R. K. Jaganatharaja, M. J. de Boer, J. W. Berenschot, M. L. Kolster, T. S. J. Lammerink, R. J. Wiegerink, and G. J. M. Krijnen. Advancements in technology and design of biomimetic flow-sensor arrays. In *22nd IEEE International Conference on Micro Electro Mechanical Systems (MEMS 2009), Sorrento, Italy*, number CFP09MEM-USB, pages 152–155, Piscataway, January 2009. IEEE Computer Society Press.

[4] Dustin W. Carr, Stephane Evoy, Lidija Sekaric, H. G. Craighead, and J. M. Parpia. Parametric amplification in a torsional microresonator. *Applied Physics Letters*, 77(10):1545–1547, September 2000.

[5] T. Shimozawa, T. Kumagai, and Y. Baba. Structural scaling and functional design of the cercal wind-receptor hairs of cricket. *J. of Comp. Physiol. A*, 183:171–186, 1998.

[6] G. Floquet. Sur les équations différentielles linéaires à coefficients périodiques. *Annales scientifiques de l'É.N.S.*, 12:47–88, 1883.